NJC

Accepted Manuscript

This is an *Accepted Manuscript*, which has been through the Royal Society of Chemistry peer review process and has been accepted for publication.

Accepted Manuscripts are published online shortly after acceptance, before technical editing, formatting and proof reading. Using this free service, authors can make their results available to the community, in citable form, before we publish the edited article. We will replace this *Accepted Manuscript* with the edited and formatted *Advance Article* as soon as it is available.

You can find more information about *Accepted Manuscripts* in the Information for Authors.

Please note that technical editing may introduce minor changes to the text and/or graphics, which may alter content. The journal's standard Terms & Conditions and the Ethical guidelines still apply. In no event shall the Royal Society of Chemistry be held responsible for any errors or omissions in this *Accepted Manuscript* or any consequences arising from the use of any information it contains.

ROYAL SOCIETY OF CHEMISTRY

www.rsc.org/njc

Effect of anion substitution on hydration, ionic conductivity and mechanical properties of anion-exchange membranes.

L. Pasquini [a,b,c], M. L. Di Vona [b*,c], P. Knauth [a,c]

[a] *Aix Marseille Université (AMU), CNRS, Madirel, UMR 7246, Campus St Jérôme, F-13397 Marseille, France*

[b] *Università di Roma Tor Vergata (URoma2), Dipartimento di Ingegneria Industriale, I-00133 Roma, Italy*

c International Associated Laboratory (L.I.A.): Ionomer Materials for Energy (AMU, URoma2, CNRS)

Abstract

Anion-conducting ionomers were synthesized by chloromethylation of polysulfone (PSU) followed by formation of quaternary ammonium groups by reaction with trimethylamine (TMA) or 1,4-diazabicyclo[2.2.2]octane (DABCO). The degree of functionalization was determined by ^{1}H NMR and titration. The anions (F^-, Cl^-, Br^-, SO_4^{2-}, NO_3^-, CO_3^{2-}, HCO_3^-, $CH_3CO_2^-$, OH^-) were substituted by ion exchange in aqueous solution. The water uptake, ionic conductivity and mechanical properties of the various ionomers were determined. The hydration has a large influence on both ionic conductivity and mechanical properties: the ionic conductivity increases with the water uptake, whereas the Young modulus decreases. Hydroxide and fluoride containing ionomers present a particularly large ionic conductivity.

Keywords: Solid ion conductors; Polymer electrolytes; Water uptake; Young modulus

Graphical abstract

Ionic conductivity and mechanical properties of ionomers with various anions

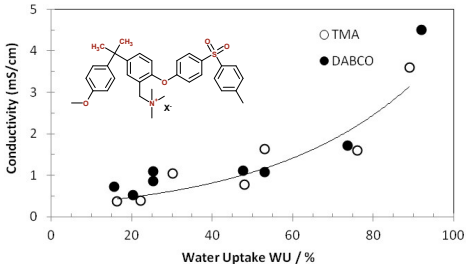

Introduction

Anion conducting polymers [1] have many potential applications, such as anion exchange membranes [2], electrodialysis [3, 4] and water purification [5], or electrochemical energy technologies, such as alkaline fuel cells [6-14], water electrolysis [15], and redox flow batteries [16, 17]. Key figures of merit of ionomers for all these applications are hydration, ionic conductivity and mechanical properties.

In order to obtain an electrolytic polymer with selective anion transport, it is necessary to graft the cationic groups on the macromolecular chains so that only the anions are mobile in the electric field. Only few cationic groups have been described so far, including ammonium, sulfonium and phosphonium [18-20]. However, among these, only ammonium groups present sufficient stability for use in aggressive environment [21, 22]. One favorite way to obtain quaternary ammonium groups is to chloromethylate an aromatic polymer with successive reaction with a tertiary amine [23-25]. The counter-ion can be varied by ion exchange in solution [26-28].

From a fundamental point of view, it is interesting to study which factors have a prime influence on the transport of various anions inside ionomers, including the water uptake, the intrinsic anion mobility or the type of ammonium cation. From an application point of view, the mechanical properties are of great importance, because they determine to some extent the usefulness and durability of the prepared membranes [29].

In this contribution, we have determined the water uptake, ionic conductivity and mechanical properties of various anion-conducting ionomers based on polysulfone with quaternary ammonium groups using trimethylamine or 1,4-diazabicyclo[2.2.2]octane (DABCO) as tertiary amines. Various anions were introduced by an ion exchange procedure. The water uptake and ionic conductivity data are analyzed in terms of anion mobility. Given the interdependence of stiffness and hydration in ionomers, the mechanical properties were analyzed as function of the type of anion and hydration.

Experimental

1.1. Products

Polysulfone (PSU, MW = 55500 g/mol) was purchased from Solvay. Stannic chloride ($SnCl_4$), sodium fluoride, paraformaldehyde ($(CH_2O)_n$), trimethylchlorosilane, trimethylamine (TMA, 4.2

M in ethanol) and 1,4-diazabicyclo[2.2.2]octane (DABCO) were reagent grade and were used as received from Aldrich.

1.2. Polymer synthesis

Chloromethylation of PSU (CMPSU)

The chloromethylation reaction of PSU is shown in Scheme 1 [25]. In short, PSU (3.78 g, 8.55 meq) was dissolved in chloroform (410 mL) under nitrogen flux giving a 0.021 M solution. After dissolution, paraformaldehyde (2.57 g, 85.5 meq) and trimethylchlorosilane (10.8 mL, 85.5 meq) were added. Then $SnCl_4$ (0.1 mL in 50 mL of chloroform, 1.71 meq) was slowly introduced. The reaction was left under stirring at 55°C for 100 h. The solution was then cooled to RT and precipitated in ethanol. The product (CMPSU) was dried overnight at 60°C. The final DCM was 1.20. ^{1}H NMR spectra were recorded with a Bruker Avance 300 spectrometer operating at 300.13 MHz. Chemical shifts (ppm) are referenced to tetramethylsilane (TMS). DMSO-d6 was used as solvent.

Amination of CMPSU

PSU-TMA (trimethylamine)

CMPSU (typically 1 meq) was dissolved in 20 mL DMSO under N_2 at RT. Then 0.48 mL of a 4.2 M solution of trimethylamine in ethanol (2 meq) was added. The solution was kept under stirring for 3 days at 70 °C, and then heated under vacuum to remove the excess of amine during 3 hours at 85 °C. The solution of PSU-TMA in DMSO (0.05 M) was directly used for the casting procedure. A little quantity was dried and then analyzed by ^{1}H NMR using DMSO-d6 as solvent.

PSU-DABCO (1,4-diazabicyclo[2.2.2]octane)

A similar procedure was followed for the synthesis of the DABCO derivative using a ratio between the quantity of chloromethyl groups and DABCO of 1:1.5. After dissolution of the two precursors, the solution was kept under stirring for 4 days at 70 °C, and then heated under high vacuum to remove the excess of amine during 3 hours at 85 °C. The solution of PSU-DABCO in

DMSO (0.05 M) was directly used for the casting procedure. A little quantity was dried and then analyzed by ^{1}H NMR using DMSO-d6 as solvent.

1.3. Casting of the membrane and ion exchange

Typically 10 mL of a 0.05 M solution in DMSO was evaporated to 5 mL, cast on a Petri dish or using a home-made doctor-blade type apparatus, then heated to dryness at 100 °C for 24 h. The membrane thickness was in a range of 20 to 30 μm. In the final step, the cast membranes were immersed 24 h at 25 °C into 1 M solution of various sodium salts, including NaF, NaCl, NaBr, Na_2SO_4, $NaNO_3$, Na_2CO_3, $NaHCO_3$, CH_3CO_2Na and NaOH, and thoroughly washed several times in deionized water.

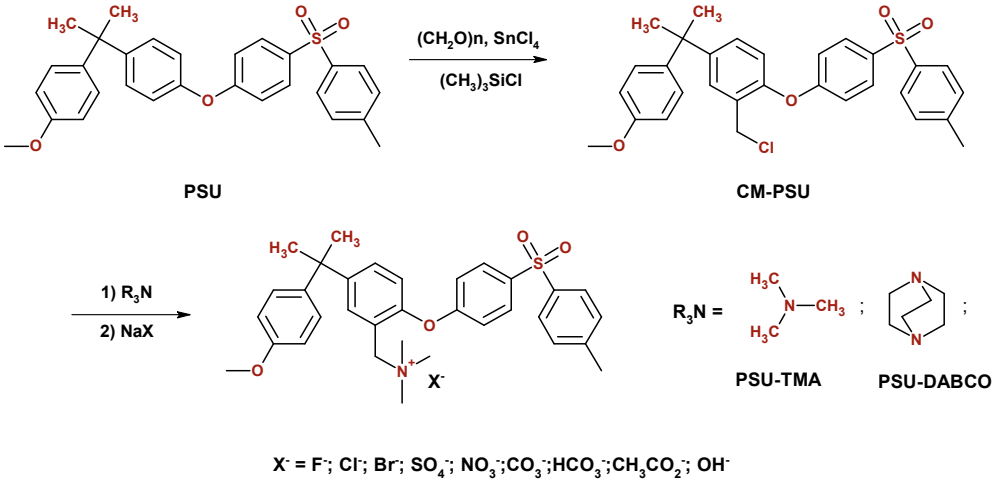

Scheme 1. Synthesis route for PSU-TMA and PSU-DABCO ionomers.

1.4. IEC and Water Uptake measurements

The Ionic Exchange Capacity (*IEC,* in equivalents per kg of dry polymer) of the ionomers was determined indirectly by NMR, measuring the degree of amination (Figure 1), and directly by acid-base titration. In the last case, after the exchange with OH^- ions, the membranes were washed in deionized water and dried over P_2O_5 for 3 days. The samples were weighted and

immersed in a 0.1 N HCl solution. The acidic solution was then back-titrated with 0.1 N NaOH with potentiometric equivalent point detection. The IEC were 1.64 and 1.25 eq/Kg for PSU-TMA and PSU-DABCO respectively.

The water uptake *WU* was measured by full immersion of membrane samples in deionized water at 25 °C: polymer samples were weighed before and after immersion times of 24 h. The dry mass was obtained after keeping the sample 72 h over P_2O_5.

The water uptake *WU* (in %) can be calculated from the ionomer mass in wet (m_{wet}) and dry (m_{dry}) conditions, according to:

$$WU = \frac{m_{wet} - m_{dry}}{m_{dry}} \times 100 \qquad (1)$$

1.5. Impedance spectroscopy (through-plane measurements)

The ionic conductivity was measured after carefully washing the membranes in deionized water to remove any excess of sodium salts. All measurements were made at 25 °C in fully humidified conditions. The ionic conductivity was measured by impedance spectrometry (EG&G model 6310) in a Swagelok cell with stainless steel electrodes; the AC voltage amplitude was 20 mV and the frequency range 1-10^5 Hz. The through-plane membrane resistance *R* was determined from the high frequency intersection of the impedance arc with the real axis in a Nyquist plot. The anion conductivity σ was calculated from the membrane thickness *d* and the electrode area, which was A = 0.264 cm^2, using the equation:

$$\sigma = \frac{d}{R \cdot A} \qquad (2)$$

1.6 Mechanical measurements

Tensile stress-strain tests were performed using an ADAMEL Lhomargy DY30 traction machine at 25°C at a constant crosshead speed of 5 mm/min. Particular attention was given to the macroscopic homogeneity of membranes made by casting and only apparently homogeneous membranes were used for the mechanical tests. The membrane samples had a thickness of 20-30 μm, 5 mm width and 25 mm length. The border of the membranes, where composition may be inhomogeneous, was eliminated by cutting carefully the specimens. The selected tensile curves corresponded only to tests with a final rupture in the central part of the specimens. The other

cases of rupture, e.g., near or under grips, were systematically eliminated. Prior to the measurements, the polymer samples were stabilized at 25 °C and humidity (40±10)% RH. The measurement time was below 5 min.

Results

The chloromethylation reaction is made in a friendly way, because the toxic chloromethylating agent is formed in situ and destroyed during the precipitation step in ethanol. The reaction is carried out in diluted conditions (0.021 M) to avoid the reticulation due to the Friedel-Crafts attack of the chloromethyl moiety on an unsubstituted phenyl ring.

The amination reaction is shown in Scheme 1 [25]. Chloromethylated PSU is the starting reagent for the formation of quaternary ammonium groups via a S_N2 reaction with trimethylamine or DABCO. Due to the presence of two nucleophilic sites in the DABCO structure, it is possible during the quaternization reaction to obtain cross-linked membranes. However, when an equimolar ratio (or more) of CH_2Cl derivative and DABCO is used, it is possible to avoid the cross-linking reaction [2].

Figure 1a reports the ^1H spectrum of CMPSU with DCM = 1.2. A complete assignment of the spectrum was performed and the letters on the spectrum correspond to the proton positions. The ratio between the area of protons A at 7.9 ppm (4 H) and F at 4.5 ppm (2 H) gives the degree of chloromethylation.

Figure 1b shows the ^1H NMR spectrum of PSU-$CH_2N(CH_3)_3^+Cl^-$. The signal of the $N(CH_3)_3$ moiety appears at 3.1 ppm, while the peaks due to the CH_2N group, centred at 4.6 ppm, are split and shifted with respect to the absorption of the CH_2Cl moiety of the chloromethyl derivative. The splitting shows the non-equivalence of the two protons that feel different environments due to the presence of three bulky methyl groups.

The degree of amination (DAM) is calculated by the ratio between the area of protons A at 7.9 ppm (4 H) and protons of $N^+(CH_3)_3$ moiety at 3.1 ppm (DAM = 0.86). This corresponds to an IEC of 1.70 eq/kg in good agreement with the value estimated by titration.

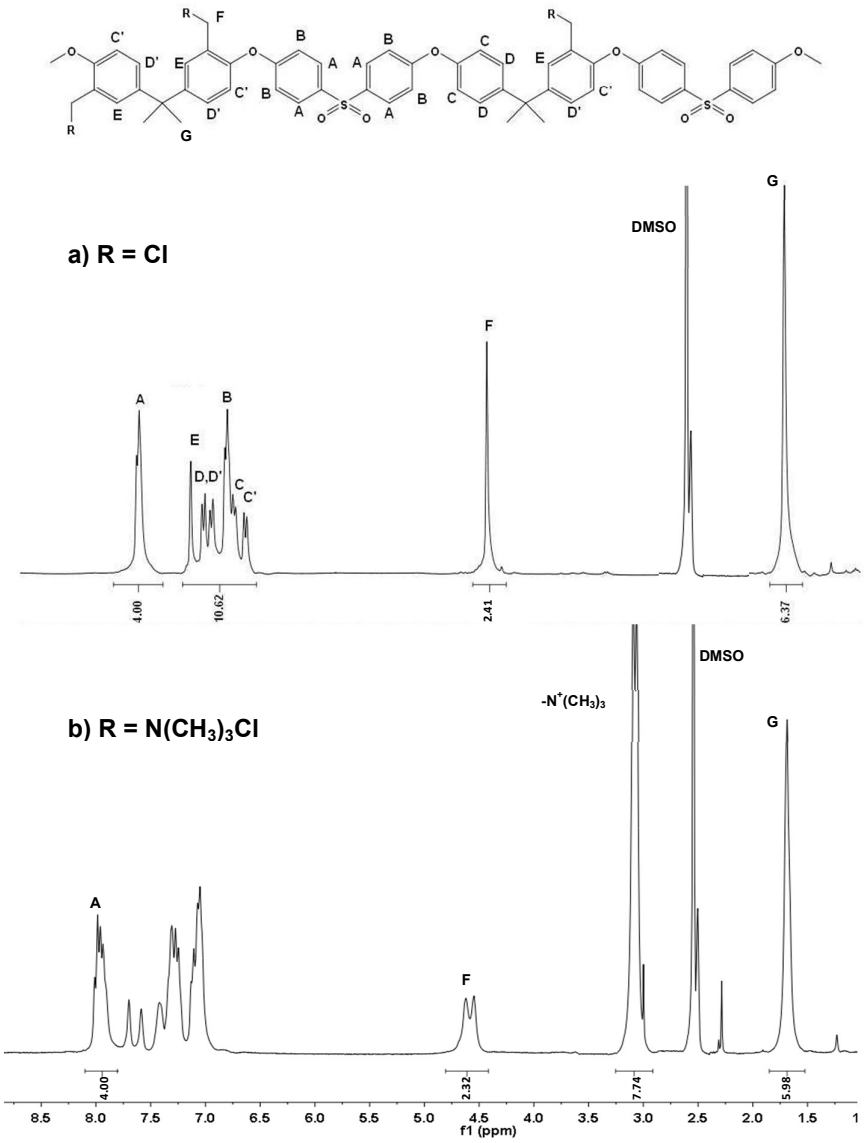

Figure 1. [1]H NMR spectra in DMSO-d6 of a) CMPSU and b) PSU-TMA

The water uptake and ionic conductivity data for the various anion-exchanged membranes are reported in Table 1. The water uptake is quite similar for TMA and DABCO-functionalized ionomers. In general, anions are less solvated than cations [30]. A particularly large water uptake is observed for hydroxide, fluoride and acetate ions. In the case of acetate ions, this result is consistent with the large ion hydration reported in the literature [31, 32].

Concerning the conductivity data, the large value for hydroxide ions was anticipated, given its particular diffusion mechanism in aqueous media. One notices also the relatively high conductivity of fluoride ions, which is related to the large hydration of the small fluoride ion that

forms particularly strong hydrogen bonds. We have recently determined by ^{19}F NMR pulse gradient spin echo spectroscopy, the F^- ion self-diffusion coefficient, which is consistent with the ionic conductivity [33].

We investigated also carbonate and hydrogencarbonate anions. These anions are also formed when hydroxide-containing ionomers are in contact with the atmosphere. They are related by an acid-base equilibrium shifted according to the acidic constant of hydrogencarbonate (pKa_2 = 10.3); the conversion between hydrogencarbonate and carbonate is thus very limited. In fact, although the water uptake is similar, the ionic conductivity and mechanical properties of the ionomers are quite different.

The ionic conductivity of all TMA and DABCO-based ionomers with various anions is shown in Figure 2 as function of the water uptake. The conductivity does evidently depend much on the hydration; the line is to guide the eye.

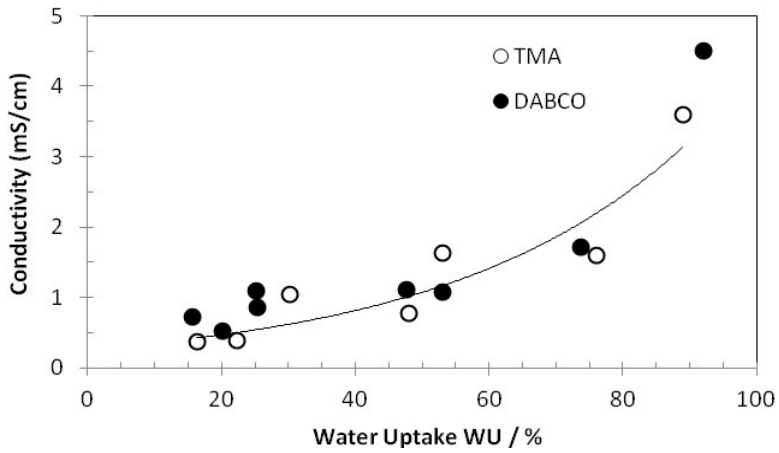

Figure 2. Anion conductivity of ionomers based on PSU-TMA and PSU-DABCO with various anions as function of the water uptake.

Typical tensile stress-strain test curves are shown for PSU-TMA and PSU-DABCO membranes with various anions in Figure 3. The mechanical properties (Young modulus and tensile strength) are reported for all investigated ionomers in Table 1. One can observe a similar elasto-plastic behavior for all ionomers with a Young modulus between 0.6 and 1.5 GPa, which is strongly correlated with the water uptake of the membrane, and a tensile strength within a range 20-50 MPa. Altogether, these membranes behave as relatively stiff and strong polymers, in accordance with the large amount of ionic groups.

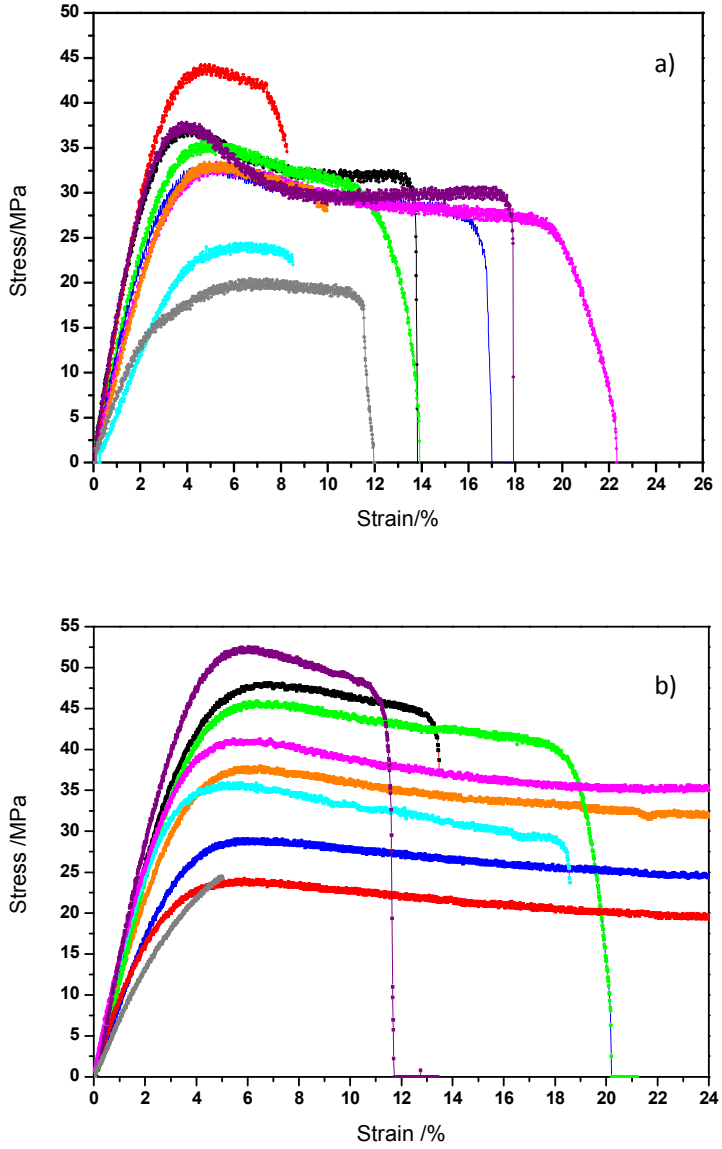

Figure 3. Typical tensile stress-strain curves for anion-conducting a) PSU-TMA and b) PSU-DABCO ionomers. ● HCO_3^-; ● CO_3^{2-}; ● $CH_3CO_2^-$; ● NO_3^-; ● SO_4^{2-}; ● F^-; ● Cl^-; ● Br^-; ● OH^-.

Discussion

The mechanical properties, especially the Young modulus, are strongly related to the water uptake.

Figure 4 shows a plot of the Young modulus versus the water uptake with a tentative linear regression line. The elastic modulus, which is related to the Van der Waals interactions between the macromolecular chains, decreases very strongly when the water uptake increases. The high dielectric constant of water decreases significantly the interactions among macromolecules and weakens considerably the stiffness of the ionomer. Similar results have already been reported for Nafion, where an inverse relationship between elastic modulus and hydration number was observed [34], and for sulfonated poly (ether ether ketone) [35].

Ion-specific interactions with macromolecules, such as those discussed in the Hofmeister series [36, 37], play certainly also a role. The Hofmeister series ranks the relative influence of ions on the physical behavior of a wide variety of aqueous processes ranging from colloidal assembly to protein folding. Such effects are generally more pronounced for anions than for cations. For anion exchange membranes, which present a positive Donnan potential, swelling is highly dependent on the type of anion, whereas cations have no significant influence [37]. Fluoride and acetate ions belong to the so-called "cosmotropes" [36], which are strongly hydrated and stabilize macromolecules. Recent experiments indicate that highly specific ion-macromolecule interactions, as well as with water molecules in the first hydration shell, including Van der Waals and ion-dipole forces, are responsible for most phenomena [36]. Although Hofmeister effects for macromolecules in aqueous solution are ubiquitous, the molecular-level mechanisms by which ions operate are still matter of study and debate [38].

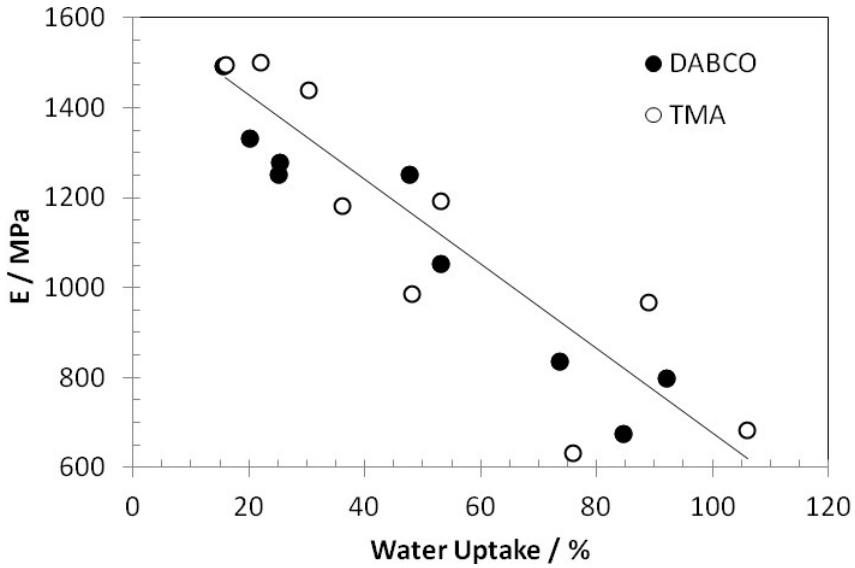

Figure 4. Young modulus versus water uptake for PSU-TMA and PSU-DABCO with various anions.

The concentration *c* of the electrolytic solutions (in mol/L) inside the ionomer can be estimated using equation (3), established for proton-conducting ionomers [39, 40], using the *IEC* of the ionomer and the water uptake *WU*. The density ρ of the electrolytic solution is assumed to be 1 kg/L; Alberti and coworkers determined the density of electrolytic solutions inside Nafion and found in fact values in the order of unity [41].

$$c = \frac{IEC \cdot \rho}{WU} * 100 \qquad (3)$$

The assumptions are that all ionic groups are dissociated and that the water is completely inside the hydrated channels. One should recall that sulfonic acid groups in acidic polymers can be undissociated at low water content; in anion conducting ionomers, the quaternary ammonium groups are always dissociated, but ion pairs can form at low hydration.

The anion mobility $u(X^-)$ (in $cm^2\ V^{-1}\ s^{-1}$) inside the ionomer can be calculated according to equation (4), given that quaternary ammonium cations are fixed on the macromolecular chain, and do not contribute to the ionic conductivity.

$$u(X^-) = \frac{\sigma}{z \cdot F \cdot c} \qquad (4)$$

In this equation, σ is the anion conductivity (in mS/cm), z is the charge of the anion and *F* is Faraday's constant.

Figure 5 shows the anion mobility data plotted against the square root of the anion concentration. The best fitting of the data, obtained for various anions, is obtained with a power law $u(X^-) \sim A.c^{-3}$ (see regression line).

A similar law was found previously for proton-conducting sulfonated aromatic polymers; this law can be related to the "universal" power law observed near the percolation threshold for a three-dimensional network of ion conducting hydrated channels [42-46]. A quite similar behavior is thus observed for anion-conducting ionomers; the percolation of hydrated channels and the level of hydration play evidently a very important role whatever the anion and their intrinsic mobility.

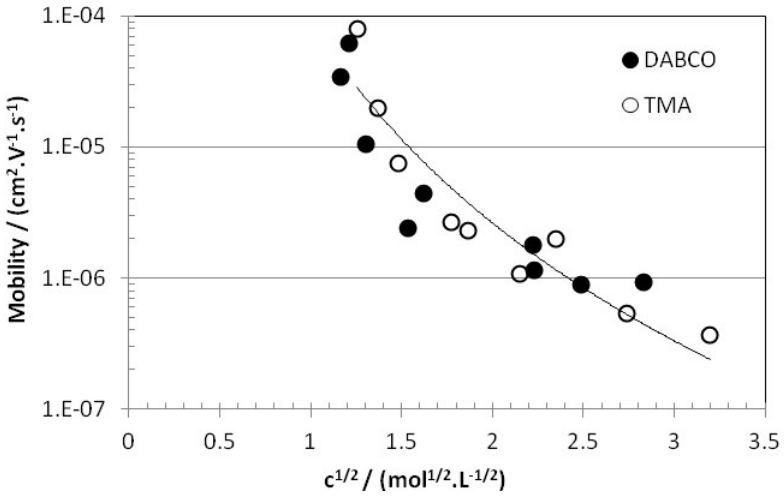

Figure 5. Anion mobility as function of the square root of concentration calculated according to equation (3).

The percolation threshold is related to the tortuosity, shape, size and connectivity of the hydrated ion conduction channels inside the ionomer [44]. More tortuous and less connected nanochannels percolate at a higher volume fraction of the aqueous phase [44]. The lower nanophase separation assumed in AEM [1] in comparison with proton exchange membranes can be related to the lower hydration of anions vs protons and the lower hydrophilicity of quaternary ammonium vs sulfonic acid groups.

The percolation threshold, which is detected in proton-conducting sulfonated aromatic polymers by a brutal drop of the proton mobility for a proton concentration higher than 10 mol/L [39, 47], is apparently not observed in the hydration range explored here (Figure 5). In fact, the domain of very high concentration that could be observed in proton-conducting ionomers is not accessible here, given the lower IEC of anion conducting ionomers.

Conclusion

We have prepared various anion-conducting ionomers based on PSU with quaternary ammonium groups using TMA and DABCO. The anions are substituted by ionic exchange. The anion conductivity and the mechanical properties are correlated with the ionomer hydration. AEM are ionomers with high ionic character and high stiffness, but relatively low ionic conductivity. The stiffness of the membrane, which is related to the high ionic character and rigid aromatic

backbone, decreases with the hydration, whereas the ionic conductivity, related to the low anion mobility and the apparently tortuous and low connectivity hydrated channels, increases with the water uptake. The increase of the anion mobility with decreasing anion concentration follows a power law, which is quite similar to that observed in proton-conducting ionomers and can be related to the universal behavior near the percolation threshold of hydrated channels. The conductivity of hydroxide and fluoride-ion conductors is particularly high, related to a large hydration.

The relation between membrane properties and the anion type is complex; for example the hydration of the ionomer in presence of anions is different from the anion hydration in water. It depends on the dispersion forces and ion-dipole interactions between macromolecule, water and anion. Given that the hydration is a determining parameter for electrical and mechanical properties, it is evident that a better understanding of these interactions should open the way to the development of optimized high performance anion exchange ionomers.

ACKNOWLEDGMENTS

LP acknowledges the financial support from the Franco-Italian University (Vinci Program).

Table 1. Water uptake WU, ionic conductivity σ, Young modulus E, and tensile strength TS of anion-exchange membranes with various anions and with the two amines.

	TMA				DABCO			
SALT	WU / %	σ / mS cm^{-1}	E / MPa	TS / MPa	WU / %	σ mS cm^{-1}	E / MPa	TS / MPa
NaOH	106	12.0	683	20	85	8.8	675	25
NaF	89	3.6	966	33	92	4.5	799	24
NaCl	30	1.1	1438	44	25	0.9	1277	39
NaBr	16	0.4	1495	38	20	0.5	1333	48
Na_2SO_4	36	1.0	1182	33	25	1.1	1252	46
$NaNO_3$	22	0.4	1501	38	16	0.7	1494	52
Na_2CO_3	53	1.6	1191	36	53	1.1	1054	38
$NaHCO_3$	48	0.8	985	33	48	1.1	1253	41
CH_3CO_2Na	76	1.6	631	24	74	1.7	836	29

Captions

Scheme 1. Synthesis route for PSU-TMA and PSU-DABCO ionomers.

Figure 1. ^{1}H NMR spectra in DMSO-d6 of a) CMPSU and b) PSU-TMA

Figure 2. Anion conductivity of ionomers based on PSU-TMA and PSU-DABCO with various anions as function of the water uptake.

Figure 3. Typical tensile stress-strain curves for anion-conducting a) PSU-TMA and b) PSU-DABCO ionomers. ● HCO_3^-; ● CO_3^{2-}; ● $CH_3CO_2^-$; ● NO_3^-; ● SO_4^{2-}; ● F^-; ● Cl^-; ● Br^-; ● OH^-.

Figure 4. Young modulus versus water uptake for PSU-TMA and PSU-DABCO with various anions.

Figure 5. Anion mobility as function of the square root of concentration calculated according to equation (3).

References

1. M. A. Hickner, A. M. Herring and E. B. Coughlin, *Journal of Polymer Science Part B-Polymer Physics*, 2013, **51**, 1727-1735.
2. B. Bauer, H. Strathmann and F. Effenberger, *Desalination*, 1990, **79**, 125-144.
3. X. M. Yan, G. H. He, X. M. Wu and J. Benziger, *Journal of Membrane Science*, 2013, **429**, 13-22.
4. A. Elattar, A. Elmidaoui, N. Pismenskaia, C. Gavach and G. Pourcelly, *Journal of Membrane Science*, 1998, **143**, 249-261.
5. M. A. Hickner, *Materials Today*, 2013, **13**, 34-41.
6. J. R. Varcoe and R. C. T. Slade, *Fuel Cells*, 2005, **5**, 187-200.
7. J. Fang and P. K. Shen, *Journal of Membrane Science*, 2006, **285**, 317-322.
8. J. Jagur-Grodzinski, *Polymers for Advanced Technologies*, 2007, **18**, 785-799.
9. G. Couture, A. Alaaeddine, F. Boschet and B. Ameduri, *Progress in Polymer Science*, 2011, **36**, 1521-1557.
10. G. Merle, M. Wessling and K. Nijmeijer, *Journal of Membrane Science*, 2011, **377**, 1-35.
11. J. Zhou, J. S. Guo, D. Chu and R. R. Chen, *Journal of Power Sources*, 2012, **219**, 272-279.
12. Y. J. Wang, J. L. Qiao, R. Baker and J. J. Zhang, *Chemical Society Reviews*, 2013, **42**, 5768-5787.
13. E. Agel, J. Bouet and J. F. Fauvarque, *Journal of Power Sources*, 2001, **101**, 267-274.
14. L. An, T. S. Zhao, Q. X. Wu and L. Zeng, *International Journal of Hydrogen Energy*, 2012, **37**, 14536-14542.
15. S. Marini, P. Salvi, P. Nelli, R. Pesenti, M. Villa, M. Berrettoni, G. Zangari and Y. Kiros, *Electrochimica Acta*, 2012, **82**, 384-391.
16. Z. G. Yang, J. L. Zhang, M. C. W. Kintner-Meyer, X. C. Lu, D. W. Choi, J. P. Lemmon and J. Liu, *Chemical Reviews*, 2011, **111**, 3577-3613.
17. K. D. Kreuer, *Chemistry of Materials*, 2014, **26**, 361-380.
18. B. Qiu, B. C. Lin, L. H. Qiu and F. Yan, *J. Mater. Chem.*, 2012, **22**, 1040-1045.
19. B. Zhang, S. Gu, J. Wang, Y. Liu, A. M. Herring and Y. Yan, *RSC Adv.*, 2012, **2**, 12683-12685.
20. S. Maurya, S.-H. Shin, M.-K. Kim, S.-H. Yun and S.-H. Moon, *J. Membr. Sci.*, 2013, **443**, 28-35.
21. A. D. Mohanty and C. Bae, *Journal of Materials Chemistry A*, 2014, **2**, 17314-17320.
22. C. R. Yang, S. L. Wang, W. J. Ma, L. H. Jiang and G. Q. Sun, *J. Membr. Sci.*, 2015, **487**, 12-18.
23. G. G. Wang, Y. M. Weng, D. Chu, R. R. Chen and D. Xie, *Journal of Membrane Science*, 2009, **332**, 63-68.
24. A. Jasti, S. Prakash and V. K. Shahi, *Journal of Membrane Science*, 2013, **428**, 470-479.
25. M. L. Di Vona, R. Narducci, L. Pasquini, K. Pelzer and P. Knauth, *International Journal of Hydrogen Energy*, 2014, **39**, 14039-14049.
26. G. M. Geise, L. P. Falcon, B. D. Freeman and D. R. Paul, *Journal of Membrane Science*, 2012, **423**, 195-208.
27. R. Narducci, M. L. Di Vona and P. Knauth, *Journal of Membrane Science*, 2014, **465**, 185-192.
28. K. D. Kreuer, A. Wohlfarth, C. C. de Araujo, A. Fuchs and J. Maier, *Chemphyschem*, 2011, **12**, 2558-2560.
29. H. Y. Hou, M. L. Di Vona and P. Knauth, *Chemsuschem*, 2011, **4**, 1526-1536.
30. P. A. Bergstrom, J. Lindgren and O. Kristiansson, *Journal of Physical Chemistry*, 1991, **95**, 8575-8580.

31. H. M. A. Rahman, G. Hefter and R. Buchner, *Journal of Physical Chemistry B*, 2012, **116**, 314-323.
32. M. V. Fedotova and S. E. Kruchinin, *Journal of Molecular Liquids*, 2011, **164**, 201-206.
33. L. Pasquini, F. Ziarelli, S. Viel, M. L. Di Vona and P. Knauth, *Chemphyschem*, 2015, **16**, 3631-3636.
34. G. Alberti, R. Narducci and M. Sganappa, *Journal of Power Sources*, 2008, **178**, 575-583.
35. H. Y. Hou, B. Maranesi, J. F. Chailan, M. Khadhraoui, R. Polini, M. L. Di Vona and P. Knauth, *Journal of Materials Research*, 2012, **27**, 1950-1957.
36. Y. J. Zhang and P. S. Cremer, *Current Opinion in Chemical Biology*, 2006, **10**, 658-663.
37. R. Zahn, J. Voros and T. Zambelli, *Current Opinion in Colloid & Interface Science*, 2010, **15**, 427-434.
38. B. W. Ninham, T. T. Duignan and D. F. Parsons, *Current Opinion in Colloid & Interface Science*, 2011, **16**, 612-617.
39. P. Knauth and M. L. Di Vona, *Solid State Ionics*, 2012, **225**, 255-259.
40. M. L. Di Vona, L. Pasquini, R. Narducci, K. Pelzer, A. Donnadio, M. Casciola and P. Knauth, *Journal of Power Sources*, 2013, **243**, 488-493.
41. G. Alberti, M. L. Di Vona and R. Narducci, *International Journal of Hydrogen Energy*, 2012, **37**, 6302-6307.
42. P. Knauth, L. Pasquini, B. Maranesi, K. Pelzer, R. Polini and M. L. Di Vona, *Fuel Cells*, 2013, **13**, 79-85.
43. M. Eikerling, A. A. Kornyshev and U. Stimming, *Journal of Physical Chemistry B*, 1997, **101**, 10807-10820.
44. X. M. Wu, X. W. Wang, G. H. He and J. Benziger, *Journal of Polymer Science Part B-Polymer Physics*, 2011, **49**, 1437-1445.
45. J. P. Clerc, G. Giraud, J. M. Laugier and J. M. Luck, *Advances in Physics*, 1990, **39**, 191-308.
46. D. Staufer and A. Aharony, *Introduction to Percolation Theory*, Taylor and Francis, London, 1992.
47. P. Knauth, E. Sgreccia, A. Donnadio, M. Casciola and M. L. Di Vona, *Journal of the Electrochemical Society*, 2011, **158**, B159-B165.